

## Peculiarities of formation of a potential barrier in a dispersed medium of a two-phase dispersed system based on $ZrO_2$ and $Ca_6H_2O_{19}Si_6$

Yu.Yu. Bacherikov<sup>1,2\*</sup>, O.B. Okhrimenko<sup>1\*</sup>, A.G. Zhuk<sup>1</sup>, V.V. Ponomarenko<sup>1</sup>, D.V. Pekur<sup>1</sup>, I.A. Danilenko<sup>3</sup>, A.I. Lyubchik<sup>4</sup>, S.I. Lyubchik<sup>4</sup>

<sup>1</sup>V. Lashkaryov Institute of Semiconductor Physics, NAS of Ukraine, 41 Nauky Avenue, 03028 Kyiv, Ukraine

<sup>2</sup>V. Vernadsky Institute of General and Inorganic Chemistry, NAS of Ukraine,

32/34 Academician Palladin Avenue, 03142 Kyiv, Ukraine

<sup>3</sup>O. Galkin Donetsk Institute for Physics and Engineering, NAS of Ukraine, 46 Nauky Avenue, 03028 Kyiv, Ukraine

<sup>4</sup>DeepTechLab, RCM2+. Universidade Lusófona, Campo Grande, 376, Lisboa 1749-024, Portugal

Corresponding authors e-mail: yuyu@isp.kiev.ua, olga@isp.kiev.ua

**Abstract.** In this paper, a current-voltage characteristics method is used to study the peculiarities of formation of a potential barrier in a dispersed medium of a two-phase dispersed system based on  $ZrO_2$  and  $Ca_6H_2O_{19}Si_6$ . Using the obtained experimental data, a possibility of creating diode structures based on two-phase dispersed systems is confirmed. The configuration of the interface between the dispersed phases of the two-layer structure is shown to define the parameters of the potential barrier in a dispersed medium.

**Keywords:** current-voltage characteristics, two-layer structure, potential barrier, dispersed system.

<https://doi.org/10.15407/spqeo28.01.019>

PACS 66.10.Ed, 82.45Gj, 84.32.Ff

Manuscript received 04.01.25; revised version received 21.02.25; accepted for publication 12.03.25; published online 26.03.25.

### 1. Introduction

Research in the field of current flow in dispersed systems [1–4] as well as study of current flow processes in electrolytes and superionic conductors stimulated emergence of a concept of solid state ionics [5, 6] and led to a need to form a new concept, semiconductor ionics [7]. Semiconductor ionics as a new area of intersection of solid state physics and chemistry, electronics and electrochemistry, inorganic chemistry, materials science and energetics, has been developed over the past 2-3 years.

Application of basic concepts of the development of semiconductor technology to the description of current flow processes in dispersed systems, which is the essence of the semiconductor ionics concept [7, 8], allows one to develop devices with functional capabilities of classical semiconductor devices by using dispersed systems with ionic conductivity.

Moreover, presence of a greater variety of charge carriers in type 2 conductors referring to both their charge sign and magnitude allows us to expect that these carriers can be used to solve more diverse and complex problems as compared to the problems solved with devices based on materials with electronic conductivity.

It should be noted that, despite the rapid development of membrane electrochemistry and the research conducted in this area [9, 10], there are practically no works considering the processes in electrolytes from the standpoint of semiconductor electronics. At the same time, creation of porous structures filled with an electrolyte, in which potential barriers of various shapes can be formed due to the configuration of the structure, allows a transfer and more widespread use of the knowledge of semiconductor electronics in the field of the devices and technologies used in electrochemistry.

In [7, 8], in the framework of the concept of semiconductor ionics, the processes occurring in dispersed systems with ionic conductivity are described from the viewpoint of the basic concepts of semiconductor physics. In other words, dispersed systems with ionic conductivity are considered as ionic semiconductors or “type 2 semiconductors”. The basis for considering a dispersed system as a semiconductor material is the behavior of charge carriers (ions) localized in a dispersed medium. A portion of ions is localized on the surface of the particles of the dispersed phase (potential-determining ions). The ions of the opposite sign (counterions) can freely migrate in the dispersed medium (electrolyte).

It is shown in [7, 8] how use of several composite materials allows one to obtain structures with potential barriers formed in the electrolyte medium. These composites consist of a porous matrix, which includes several layers of different materials, filled with an electrolyte. Formation of the potential barriers in the electrolyte is achieved due to the differences in the properties of the dispersed phase (layers) of the matrix. This allows a control of the direction and magnitude of current flow in the systems with ionic conductivity by using these structures.

The aim of this work is to study the influence of the interface configuration in two-phase dispersed systems on formation of a potential barrier in the dispersed medium (electrolyte) of these systems.

## 2. Sample preparation and voltage measurements

In this work, dispersed systems consisting of compacted particles in the form of pressed tablets of  $ZrO_2 + 3 \text{ mol.}\% Y_2O_3$  (hereinafter  $ZrO_2$ ) and/or xonotlite ( $Ca_6H_2O_{19}Si_6$ ), saturated with atmospheric moisture were investigated. To compact the material in the form of tablets with a diameter  $d = 20 \text{ mm}$  and a height  $h \sim 2 \text{ mm}$ , xonotlite powders  $Ca_6H_2O_{19}Si_6$  and  $ZrO_2$  were compressed under a uniaxial pressure of  $\sim 10 \text{ MPa}$ .

$ZrO_2$  nanopowders were synthesized using the method of inverse co-precipitation from aqueous solutions of zirconium and yttrium chloride salts taken in a stoichiometric ratio, with an aqueous solution of ammonia at  $pH > 9$  [11]. The hydroxide was dried in a microwave oven until the weight loss ceased [11]. Calcination was carried out at the temperature of  $700 \text{ }^\circ\text{C}$  in a resistance furnace. The holding time was 2 hours [11].  $ZrO_2$  powders were a tetragonal modification of zirconium dioxide with a specific surface area of  $50 \text{ m}^2/\text{g}$ , measured using the BET method proposed by S. Brunauer, P.H. Emmett, E. Teller [12].

A quantitative analysis of the elemental composition of  $Ca_6H_2O_{19}Si_6$  obtained on a Rigaku NEXQC + fluorescence spectrometer is presented in [8].

To record the potential difference across the contacts of the structure, a Keithley 2635B precision source-meter was used. The measurement modes of the Keithley 2635B source were controlled using a computer. The potential scanning rate was  $0.05 \text{ V/s}$ . The applied potential range was  $\pm 2 \text{ V}$ . The measurements were carried out at room temperature ( $T = 295 \text{ K}$ ).

Current-voltage ( $I$ - $V$ ) characteristics were measured on single-layer  $Ca_6H_2O_{19}Si_6$  and  $ZrO_2$  structures as well as on the two-layer structures of  $Ca_6H_2O_{19}Si_6 + ZrO_2$  (1 type) obtained by pressing two layers of  $Ca_6H_2O_{19}Si_6$  and  $ZrO_2$  together, and  $Ca_6H_2O_{19}Si_6/ZrO_2$  (2 type) obtained by joint pressing of  $Ca_6H_2O_{19}Si_6$  and  $ZrO_2$  layers.  $I$ - $V$  characteristics were measured in 5–20 continuous measurement series.

When measuring the  $I$ - $V$  characteristics of the two-layer systems, the measurement series were carried out for two different modes of connecting a contact with a “zero” potential supplied from the Keithley 2635B.

In the first case, this contact was adjacent to the  $ZrO_2$  layer (“direct” connection), and in the second case, it was adjacent to the  $Ca_6H_2O_{19}Si_6$  layer (“reverse” connection). A voltage with a “–” sign was applied to the opposite contact for the  $I$ - $V$  characteristic branch in the range of 0 to  $+2 \text{ V}$  and with a “+” sign for the  $I$ - $V$  characteristic branch in the range of 0 to  $-2 \text{ V}$ .

A sample was placed as a partition in the middle of a special “climatic chamber” during measurements of  $I$ - $V$  characteristics [8]. Gold pressure contacts were located on both sides of the sample.

## 3. Results and discussion

Fig. 1 shows the  $I$ - $V$  characteristics of the  $ZrO_2$  structures at a humidity  $Rh \sim 40\%$  and  $\sim 100\%$ . It should be noted that the  $ZrO_2$  and  $Ca_6H_2O_{19}Si_6$  structures practically did not conduct electric current during dehydration (after annealing) [1].

As can be seen from Fig. 1, saturation of the  $ZrO_2$  structure with moisture leads to an increase in the current strength (approximately by 1.8–2 times) flowing through the structure. Moreover, increase in the number of current cycles at  $U = -2 \dots +2 \text{ V}$  (measurement series) through the structure leads to an insignificant decrease in the current strength in the  $ZrO_2$  based dispersed system both at  $Rh \sim 40\%$  ( $\sim 1.3$  times) and  $Rh \sim 100\%$  ( $\sim 1.14$  times). The comparison was made for current strength values at the voltage of  $\pm 2 \text{ V}$ .

A feature of the  $I$ - $V$  characteristics of the structures under study is the presence of hysteresis. This type of  $I$ - $V$  characteristics is typical for systems that are nonlinear capacitors [13]. The observed hysteresis effect can be explained by the relatively large capacity of the studied structures, which are a set of alternating layers ( $ZrO_2$  and  $H_2O$  particles) with different permittivities and may be considered as a set of capacitors connected in a mixed manner.

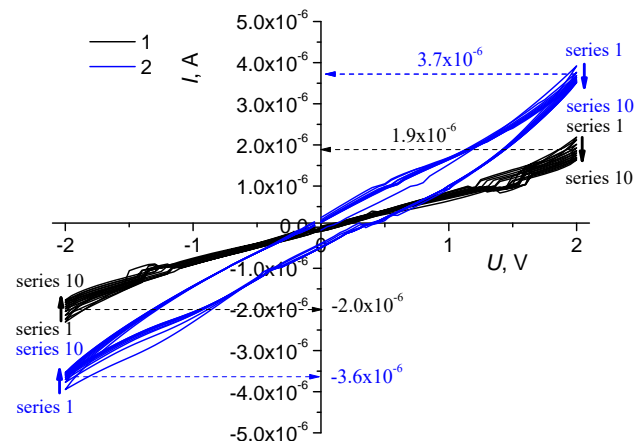


**Fig. 1.**  $I$ - $V$  characteristics of the  $ZrO_2$  structure (10 measurement series) at different humidity values: 1 –  $Rh \sim 40\%$  and 2 –  $Rh \sim 100\%$ . For interpretation of the colors in the figures, the reader is referred to the web version of this article.

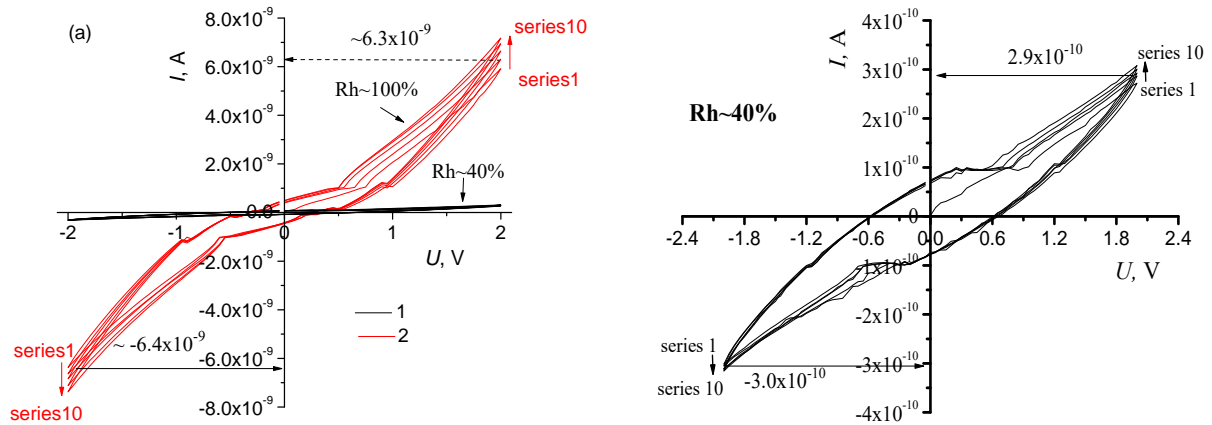


**Fig. 2.**  $I$ - $V$  characteristics of the xonotlite structure ( $\text{Ca}_6\text{H}_2\text{O}_{19}\text{Si}_6$ ) (5 measurement series) at different humidity values: 1 –  $\text{Rh} \sim 40\%$  (a, b) and 2 –  $\text{Rh} \sim 100\%$  (a).

The effect of charge accumulation on the capacitor plates, *i.e.* on the surface of the particles, is associated with the formation of a potential-determining layer due to the adsorption of water molecules and  $\text{OH}^-$  ions on the surface of the particles on the one hand and with the presence of mobile ions (protons  $\text{H}^+(\text{H}_2\text{O})_n$ ) in the diffuse layer on the other hand.

In this case, each capacitor has its own characteristic charge relaxation time (the time for the capacitor charge to decrease by  $e$  times),  $\tau = RC$ , where  $R$  is the resistance of the conductor connected to the capacitor and  $C$  is the capacitance. The hysteresis appears when the current direction changes, and the charge relaxation time  $\tau$  and the time of change in the size of the space charge region (SCR) at the interface of the particle layers are of the same order.

Since the hysteresis value remains virtually unchanged, one may conclude that the drop in the current value as it passes through the  $\text{ZrO}_2$  structure is caused by a decrease in the mobility and concentration of counterions in the dispersed system under consideration, *i.e.* protons  $\text{H}^+(\text{H}_2\text{O})_n$ .

Figs 2a and 2b show the  $I$ - $V$  characteristics of the dispersed systems based on xonotlite ( $\text{Ca}_6\text{H}_2\text{O}_{19}\text{Si}_6$ ) at different humidity values,  $\text{Rh} \sim 40\%$  and  $\sim 100\%$ . At this, Fig. 2b shows the  $I$ - $V$  characteristics of the mentioned systems at  $\text{Rh} \sim 40\%$  on an enlarged scale.

As can be seen from Fig. 2, saturation of the xonotlite structure ( $\text{Ca}_6\text{H}_2\text{O}_{19}\text{Si}_6$ ) with moisture leads to an increase in the current strength (by approximately 22-24 times) flowing through the structure, similar to the  $\text{ZrO}_2$  case (Fig. 1). For the  $\text{Ca}_6\text{H}_2\text{O}_{19}\text{Si}_6$  structure, increase in the number of measurement series insignificantly increases the current strength both at  $\text{Rh} \sim 40\%$  ( $\sim 1.1$  times) (Fig. 2b) and  $\text{Rh} \sim 100\%$  ( $\sim 1.2$  times) (Fig. 2a), in contrast to the decrease in the current strength values with an increase in the number of measurement series observed for the  $\text{ZrO}_2$  structure.

The current values were compared at the voltage of  $\pm 2$  V. In this case, the current value in the xonotlite based

structure was 3 orders of magnitude less than in the  $\text{ZrO}_2$  based structure:  $10^{-9}$  A for  $\text{Ca}_6\text{H}_2\text{O}_{19}\text{Si}_6$  and  $10^{-6}$  A for  $\text{ZrO}_2$ . It should be noted that for single  $\text{Ca}_6\text{H}_2\text{O}_{19}\text{Si}_6$  and  $\text{ZrO}_2$  structures, the  $I$ - $V$  characteristics were practically symmetrical relative to "0" and there was no current in the structures at the beginning of measurements, *i.e.* in the absence of a potential difference on the contacts, which indicates the symmetry of the connected contacts. The noted features of the  $I$ - $V$  characteristics indicate that the concentration of mobile counterions in the  $\text{Ca}_6\text{H}_2\text{O}_{19}\text{Si}_6$  structure increases as a result of several cycles of current flow through the structure, unlike the  $\text{ZrO}_2$  structure case. This is due to the fact that current flow through the  $\text{Ca}_6\text{H}_2\text{O}_{19}\text{Si}_6$  structure, *i.e.* movement of ions along the surface of the particles increases the catalytic activity of  $\text{Ca}_6\text{H}_2\text{O}_{19}\text{Si}_6$ , which activates water dissociation processes.

Fig. 3 shows the  $I$ - $V$  characteristics of the  $\text{Ca}_6\text{H}_2\text{O}_{19}\text{Si}_6 + \text{ZrO}_2$  (1 type) structure obtained by pressing  $\text{Ca}_6\text{H}_2\text{O}_{19}\text{Si}_6$  and  $\text{ZrO}_2$  layers, at the humidity values  $\text{Rh} \sim 40\%$  and  $\sim 100\%$ . As can be seen from Fig. 3, a weak rectifying effect with a coefficient of  $\sim 1.76$  for "direct" connection and  $\sim 2.21$  for "reverse" connection is observed at  $\text{Rh} \sim 40\%$ . Increasing the humidity to 100% leads to a tenfold current increase in the structure.

In this case, the rectification coefficient remains practically unchanged and is  $\sim 1.6$  for "direct" connection and  $\sim 2.22$  for "reverse" connection. The current strength in the  $\text{Ca}_6\text{H}_2\text{O}_{19}\text{Si}_6 + \text{ZrO}_2$  (1 type) structure is about  $10^{-9}$  A, which is typical by the order of magnitude of dispersed systems based on  $\text{Ca}_6\text{H}_2\text{O}_{19}\text{Si}_6$ . This may indicate the dominance of the contribution of the  $\text{Ca}_6\text{H}_2\text{O}_{19}\text{Si}_6$  structure to the integral resistance of the  $\text{Ca}_6\text{H}_2\text{O}_{19}\text{Si}_6 + \text{ZrO}_2$  (1 type) structure, caused by the mobility and concentration of mobile ions ( $\text{OH}^-$ ) in it.

Figs 4a and 4b show the  $I$ - $V$  characteristics of the double structures  $\text{Ca}_6\text{H}_2\text{O}_{19}\text{Si}_6/\text{ZrO}_2$  (2 type) obtained by joint pressing two layers of  $\text{Ca}_6\text{H}_2\text{O}_{19}\text{Si}_6$  and  $\text{ZrO}_2$  at the humidity values  $\text{Rh} \sim 40\%$  and  $\sim 100\%$ .

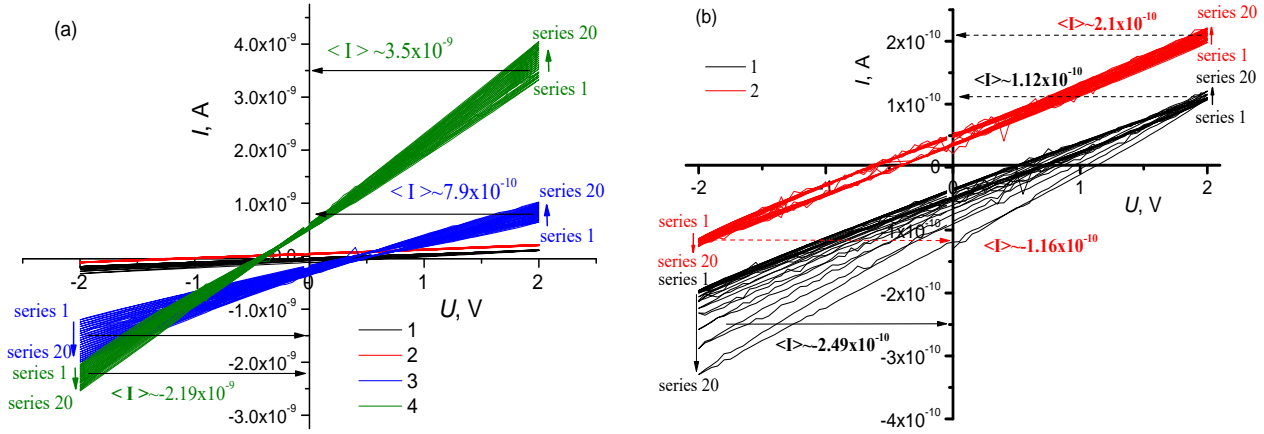


**Fig. 3.**  $I$ - $V$  characteristics of the  $\text{Ca}_6\text{H}_2\text{O}_{19}\text{Si}_6 + \text{ZrO}_2$  structure (1 type) (20 series): (a) at Rh ~ 40% (1, 2) and Rh ~ 100% (3, 4). 1, 3 – “direct” connection, 2, 4 – “reverse” connection; (b) at Rh ~ 40%. 1 – “direct” connection, 2 – “reverse” connection.

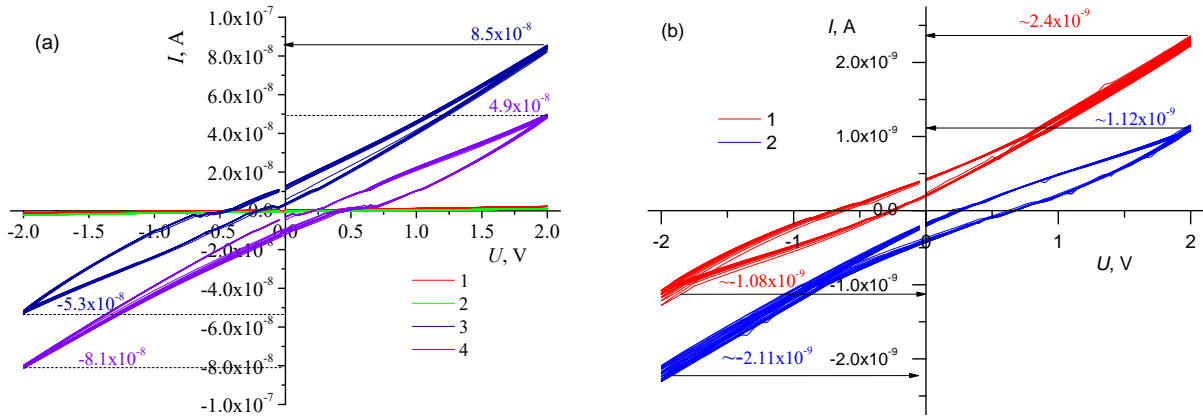


**Fig. 4.**  $I$ - $V$  characteristics of the  $\text{Ca}_6\text{H}_2\text{O}_{19}\text{Si}_6/\text{ZrO}_2$  structure (2 type) (20 series): (a) at Rh ~ 40% (1, 2) and Rh ~ 100% (3, 4). 1, 3 – “direct” connection, 2, 4 – “reverse” connection, (b) at Rh ~ 40%. 1 – “direct” connection, 2 – “reverse” connection.

As can be seen from Fig. 4b, even at the humidity of 40%, a weak rectifying effect with a coefficient of ~2.04 for “direct” connection and ~1.94 for “reverse” connection is observed in the  $\text{Ca}_6\text{H}_2\text{O}_{19}\text{Si}_6/\text{ZrO}_2$  (2 type) structure. Increasing the humidity to 100% leads to a tenfold current increase in this structure (Fig. 4a). The rectification coefficient at Rh ~ 100% is ~1.59 for “direct” connection and ~1.65 for “reverse” connection.

The current strength in the  $\text{Ca}_6\text{H}_2\text{O}_{19}\text{Si}_6/\text{ZrO}_2$  (2 type) structure is about 10<sup>-8</sup> A, which is two orders of magnitude less than that for the dispersed ZrO<sub>2</sub> based systems (~10<sup>-6</sup> A) and an order of magnitude greater than that for the dispersed systems based on Ca<sub>6</sub>H<sub>2</sub>O<sub>19</sub>Si<sub>6</sub> and Ca<sub>6</sub>H<sub>2</sub>O<sub>19</sub>Si<sub>6</sub> + ZrO<sub>2</sub> (1 type) (~10<sup>-9</sup> A). At the same time, the difference from the Ca<sub>6</sub>H<sub>2</sub>O<sub>19</sub>Si<sub>6</sub> + ZrO<sub>2</sub> (1 type) structure is that there is practically no change in the current strength with the number of measurement series at  $U = \pm 2$  V.

It should be noted that each individual layer of the structure is a dispersed system consisting of a solid porous dispersed phase – pressed particles of Ca<sub>6</sub>H<sub>2</sub>O<sub>19</sub>Si<sub>6</sub>

or ZrO<sub>2</sub>, as well as a dispersed medium – H<sub>2</sub>O. Considering that OH<sup>-</sup> groups and H<sub>2</sub>O molecules oriented depending on the sign of the surface states [3] are mainly adsorbed on the ZrO<sub>2</sub> surface, and that H<sup>+</sup> and H<sub>2</sub>O molecules are on the surface of Ca<sub>6</sub>H<sub>2</sub>O<sub>19</sub>Si<sub>6</sub>, the majority mobile charge carriers in the diffuse layer of the porous ZrO<sub>2</sub> are positively charged counterions, *i.e.* hydrated protons H<sup>+</sup>(H<sub>2</sub>O)<sub>n</sub> [3], whereas in the diffuse layer of the porous Ca<sub>6</sub>H<sub>2</sub>O<sub>19</sub>Si<sub>6</sub>, negatively charged counterions are OH<sup>-</sup> [3] (see Fig. 5).

The manifestation of the rectifying effect when current passes through a two-phase dispersed system in different directions means that there is a potential barrier in this structure. As was shown in [7], when layers of materials with different types of electrical conductivity come into contact, the gradient of charge carrier concentration causes diffusion of ions through the interface into the areas with the opposite type of electrical conductivity (Fig. 5). Due to the diffusion of charge carriers, the electrical neutrality of the areas adjacent to the interface is disrupted.

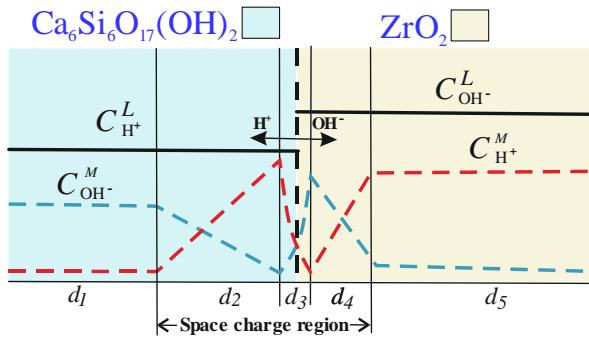


**Fig. 5.** Scheme of the distribution of ions in the  $\text{Ca}_6\text{H}_2\text{O}_{19}\text{Si}_6/\text{ZrO}_2$  structure and adjacent diffuse layers. 2, 4 – diffuse layers, 3 – anion-cation-exchange layer, 1, 5 – bulk layer.  $C_{\text{OH}^-}^L$  and  $C_{\text{H}^+}^L$  are the concentrations of fixed ion groups on the surface of the monopolar layers and  $C_{\text{OH}^-}^M$  and  $C_{\text{H}^+}^M$  are the concentrations of mobile counterions in the layer.

In a material that allows cations to pass through, uncompensated negative ions localized on the surface of the solid matrix as well as the ions supplemented by mobile anions from the anion region remain near the interface after the diffusion of positive ions from the material. In a material that allows anions to pass through, uncompensated positive immobile ions supplemented by mobile cations from the cation region remain. Hence, a space charge region consisting of two oppositely charged layers (see Fig. 5) is formed.

A diffusion electric field appears between the uncompensated opposite charges of the stationary ions. It is directed from the anion area (analogous to an  $n$ -area) to the cation one (analogous to a  $p$ -area) (Fig. 5). The resulting diffusion electric field prevents further diffusion of mobile carriers through the interface. Hence, an equilibrium state is established. A contact potential difference forms between the anion and cation areas (see Fig. 5). This contact of two dispersed systems on the surface of the dispersed phase adsorbing ions with opposite signs and different electrical conductivity types should be interpreted as an anion-cation transition.

As can be seen from the presented results, configuration of the interface between the structures (the distance between the dispersed  $\text{Ca}_6\text{H}_2\text{O}_{19}\text{Si}_6$  and  $\text{ZrO}_2$  phases) defines the parameters of the potential barrier in the dispersed medium ( $\text{H}_2\text{O}$ ) of a two-phase dispersed system. If there is a gap between these structures, which size corresponds to the distance at which the kinetic energy of the counterions with different signs is insufficient to overcome mutual attraction at their migration in such a system, their interaction will lead to formation of neutral water molecules.

These processes lead to destabilization of the potential barrier. At a smaller distance, these processes are realized only partially, which is evident from the data for the  $\text{Ca}_6\text{H}_2\text{O}_{19}\text{Si}_6 + \text{ZrO}_2$  (1 type) system (Fig. 3).

If the distance between the dispersed phases is comparable to the average pore sizes in the dispersed phases of the system, the potential barrier in this system is quite stable, which is confirmed by the  $I$ - $V$  characteristics for the  $\text{Ca}_6\text{H}_2\text{O}_{19}\text{Si}_6/\text{ZrO}_2$  (2 type) system (Fig. 4). In other words, during mutual migration of counterions in the  $\text{Ca}_6\text{H}_2\text{O}_{19}\text{Si}_6/\text{ZrO}_2$  (2 type) system (namely protons from the  $\text{ZrO}_2$  layer to the  $\text{Ca}_6\text{H}_2\text{O}_{19}\text{Si}_6$  layer, and  $\text{HO}^-$  ions in the opposite direction), the ion kinetic energy is sufficient to overcome mutual electrostatic attraction. After the counterions pass the interface, even with the loss of the kinetic energy, they become spatially separated and cannot interact with each other anymore.

#### 4. Conclusions

Based on the obtained experimental data, the assumption made in [7, 8] has been confirmed. Namely, use of several composite materials (dispersed systems), each consisting of a porous matrix (dispersed phase) filled with an electrolyte (dispersed medium), makes it possible to obtain structures with a potential barrier formed in the electrolyte medium. Obtaining of such structures is possible due to the differences in the properties of the matrix. The formed potential barrier defines the parameters of movement of ions of a certain sign (anions or cations) through these structures.

The configuration of the interface between the structures (the distance between the dispersed  $\text{Ca}_6\text{H}_2\text{O}_{19}\text{Si}_6$  and  $\text{ZrO}_2$  phases) has been shown to define the parameters of the potential barrier in the dispersed medium ( $\text{H}_2\text{O}$ ) of a two-phase dispersed system. The potential barrier is quite stable at the distances between the dispersed phases comparable to the average pore sizes in the dispersed phases of the system.

#### References

1. Bacherikov Y.Y., Lytvyn P.M., Mamykin S.V. *et al.* Current transfer processes in a hydrated layer localized in a two-layer porous structure of nanosized  $\text{ZrO}_2$ . *J. Mater. Sci.: Mater. Electron.* 2022. **33**. P. 2753–2764. <https://doi.org/10.1007/s10854-021-07481-2>.
2. Shylo A., Doroshkevich A., Lyubchik A. *et al.* Electrophysical properties of hydrated porous dispersed system based on zirconia nanopowders. *Appl. Nanosci.* 2020. **10**. P. 4395–4402. <https://doi.org/10.1007/s13204-020-01471-2>.
3. Danilenko I., Gorban O., Shylo A. *et al.* Humidity to electricity converter based on oxide nanoparticles. *J. Mater. Sci.* 2022. **57**. P. 8367–8380. <https://doi.org/10.1007/s10853-021-06657-9>.
4. Akhkozov L., Danilenko I., Podhurska V. *et al.* Zirconia-based materials in alternative energy devices – A strategy for improving material properties by optimizing the characteristics of initial powders. *Int. J. Hydrog. Energy.* 2022. **47**. P. 41359–41371. <https://doi.org/10.1016/j.ijhydene.2021.11.193>.

5. Terabe K., Tsuchiya T., Tsuruoka T. Solid state ionics for the development of artificial intelligence components. *Jpn. J. Appl. Phys.* 2022. **61**. P. SM0803.  
<https://doi.org/10.35848/1347-4065/ac64e5>.
6. Ling C. A review of the recent progress in battery informatics. *npj Computational Materials.* 2022. **8**, No 1. P. 33.  
<https://doi.org/10.1038/s41524-022-00713-x>.
7. Bacherikov Yu.Yu., Okhrimenko O.B. Principles of creating the devices that are able to control the current flow in the second class conductors. *SPQEO.* 2022. **25**. P. 137–145.  
<https://doi.org/10.15407/spqeo25.02.137>.
8. Bacherikov Yu.Yu., Okhrimenko O.B., Liubchenko O.I. *et al.* Implementation of cyclical processes in the moisture electricity generation for continuous operation. *Energy Technology.* 2024. P. 2301245.  
<https://doi.org/10.1002/ente.202301245>.
9. Pernice M.F., Qi G., Senokos E. *et al.* Mechanical, electrochemical and multifunctional performance of a CFRP/carbon aerogel structural supercapacitor and its corresponding monofunctional equivalents. *Multifunct. Mater.* 2022. **5**. P. 025002.  
<https://doi.org/10.1088/2399-7532/ac65c8>.
10. Gupta P., Mnnit R.K.S. Overview of Multi Functional Materials. In: *New Trends in Technologies: Devices, Computer, Communication and Industrial Systems.* Ed. M.J. Er. IntechOpen, 2010. Ch. 1. <https://doi.org/10.5772/10444>.
11. Shang J.Q., Lo K.Y., Quigley R.M. Quantitative determination of potential distribution in Stern–Gouy double-layer model. *Can. Geotech. J.* 1994. **31**, No 5. P. 624–636.  
<https://doi.org/10.1139/t94-075>.
12. Brunauer S., Emmett P.H., Teller E. Adsorption of gases in multimolecular layers. *J. Am. Chem. Soc.* 1938. **60**, No 2. P. 309–319.  
<https://doi.org/10.1021/ja01269a023>.
13. Unger E.L., Hoke E.T., Bailie C.D. *et al.* Hysteresis and transient behavior in current–voltage measurements of hybrid-perovskite absorber solar cells. *Energy Environ. Sci.* 2014. **7**. P. 3690–3698.  
<https://doi.org/10.1039/C4EE02465F>.

#### Authors' contributions

**Bacherikov Yu.Yu.:** key ideas, conceptualization, investigation, formal analysis, writing – review & editing.

**Okhrimenko O.B.:** key ideas, conceptualization, investigation, supervision, writing – original draft.

**Zhuk A.G.:** investigation.

**Ponomarenko V.V.:** investigation.

**Pekur D.V.:** investigation.

**Danilenko I.A.:** formal analysis, investigation.

**Lyubchyk A.I.:** validation, resources, investigation.

**Lyubchyk S.I.:** software, validation.

#### Authors and CV



**Yuriy Yu. Bacherikov**, Doctor of Sciences in Physics and Mathematics, Leading Researcher at the V. Lashkaryov Institute of Semiconductor Physics, NAS of Ukraine. Authored over 300 publications, 6 patents, and 1 monograph. The area of his scientific interests includes physics and applications of wide-band semiconductor compounds and devices based on them.  
E-mail: [yuyu@isp.kiev.ua](mailto:yuyu@isp.kiev.ua),  
<https://orcid.org/0000-0002-9144-4592>



**Olga B. Okhrimenko**, Doctor of Sciences in Physics and Mathematics, Leading Researcher at the V. Lashkaryov Institute of Semiconductor Physics, NAS of Ukraine. Authored over 140 publications, 1 patent, and 1 monograph. The area of her scientific interests includes investigation of the patterns and physical mechanisms of formation and rearrangement of defect–impurity systems in thin-film dielectric–semiconductor structures.  
E-mail: [olga@isp.kiev.ua](mailto:olga@isp.kiev.ua),  
<https://orcid.org/0000-0002-7611-4464>



**Demid V. Pekur**, PhD in Telecommunications and Radio Engineering, Deputy Head of the Optoelectronics Department, V. Lashkaryov Institute of Semiconductor Physics, NAS of Ukraine. Authored more than 55 publications and 6 patents for inventions. His research interests include development of advanced high-power lighting systems with LED cooling based on two-phase heat-transfer technology, creation of lighting systems with wide functionalities, and development of perspective optoelectronic devices.  
E-mail: [demid.pekur@gmail.com](mailto:demid.pekur@gmail.com),  
<https://orcid.org/0000-0002-4342-5717>



**Anton G. Zhuk**, PhD in Physics and Mathematics, Senior Researcher at the V. Lashkaryov Institute of Semiconductor Physics, NAS of Ukraine. Authored 46 publications and 1 patent. The area of his scientific interests includes investigation of photoelectric properties of semiconductors and nanostructured media and development of elements of electroluminescent and sensory devices.  
E-mail: [Jook.anton@gmail.com](mailto:Jook.anton@gmail.com),  
<https://orcid.org/0000-0002-6940-1836>



**Valentyna V. Ponomarenko**, Researcher at the V. Lashkaryov Institute of Semiconductor Physics, NAS of Ukraine. Candidate for a PhD degree. Authored 7 papers and 2 theses. The area of her scientific interests is properties of functional materials.

E-mail: freundlich@ukr.net,  
<https://orcid.org/0000-0001-5722-9760>



**Igor A. Danilenko**, PhD in Solid State Physics, Senior Researcher at the O. Galkin Donetsk Institute for Physics and Engineering, NAS of Ukraine. Authored over 120 publications and 4 patents. The area of his interests includes fabrication and investigation of ceramics materials, nanomaterials for different applications and composites.

E-mail: igord69@ukr.net,  
<https://orcid.org/0000-0002-0016-1045>



**Andriy I. Lyubchyk**, PhD in Chemical Engineering (New University of Lisbon, 2013), Associate Professor at the Lusofona University, Portugal, since 2021. Authored over 60 papers in peer reviewed journals. The area of his scientific expertise includes materials science and processes, nanomaterials, chemistry of surfaces

and interfaces. E-mail: p6193@ulusofona.pt,  
<https://orcid.org/0000-0002-8883-8283>



**Sergiy I. Lyubchyk**, PhD in Chemical Engineering (New University of Lisbon, 2017). Associate Professor at the Lusofona University, Portugal, since 2021. Authored over 40 papers in peer reviewed journals. Specializes in the fields of alternative energy and advanced materials research. Current

research interests include development of advanced nanomaterials, design and application, and photochemistry of advanced composites based on nanometal oxides and fullerenes. E-mail: p6349@ulusofona.pt,  
<https://orcid.org/0000-0001-6323-938>

### Особливості формування потенціального бар'єра в дисперсному середовищі двофазної дисперсної системи на основі $ZrO_2$ та $Ca_6H_2O_{19}Si_6$

Ю.Ю. Бачеріков, О.Б. Охріменко, А.Г. Жук, В.В. Пономаренко, Д.В. Пекур, І.А. Даніленко, А.І. Любчик, С.І. Любчик

**Анотація.** У цій роботі методом вольт-амперних характеристик досліджено особливості формування потенціального бар'єра в дисперсному середовищі двофазної дисперсної системи на основі  $ZrO_2$  та  $Ca_6H_2O_{19}Si_6$ . З отриманих експериментальних даних підтверджено можливість створення діодних структур з урахуванням двофазних дисперсних систем. Показано, що конфігурація межі поділу між дисперсними фазами двошарової структури визначає параметри потенціального бар'єра дисперсного середовища.

**Ключові слова:** вольт-амперні характеристики, двошарова структура, потенціальний бар'єр, дисперсна система.